

CORRECTION OF SENSOR ALIGNMENT OF ADEOS-II/GLI

T. Hashimoto^{a,*}, K. Yamamoto^a, T. Igarashi^a

^a Japan Aerospace and Exploration Agency (JAXA)/Earth Observation Research and application Center (EORC),
1-8-10, Harumi, Chuo-ku, Tokyo 104-6023, Japan
(hashi, kath, igarashi)@eorc.jaxa.jp

KEY WORDS: Photogrammetry, Geometric, Accuracy, Optical, Sensor, Correction

ABSTRACT:

The Advanced Earth Observing Satellite (ADEOS-II) was successfully launched in December 2002 by Japan Aerospace and Exploration Agency (JAXA: former NASDA). The Global Imager (GLI) onboard the ADEOS-II is an optical mechanical scanner with 36 channels and the spatial resolution of 1 km and 250m at nadir. It observes about 1,600km in width with the FOV of +/-45 degrees. The same areas are observed every 4 days. JAXA has conducted the initial checkout of GLI image properties just after the launch of the satellite. In the checkout activities, the absolute geometric accuracy was examined. The accuracy was evaluated utilizing ground control point(GCP)s which were automatically extracted by the template matching between GLI image chips and coastline database. The examination for many images showed the geometric accuracy was about a few kilo-meters on the ground. Most of the errors were static, in other words, every image has the almost same geometric errors in both amplitude and direction. Such error patterns were seemed to be induced by the miss-alignments of the GLI sensor. The authors corrected the alignments of the GLI sensor based on the collinearity condition in the photogrammetry. After the correction, the geometric accuracy was improved to about one pixel even in 250m channel images.

1. INTRODUCTION

1.1 GLI sensor

The GLI is an optical sensor which observes solar light reflected from the Earth's surface including land, ocean and cloud, or infrared radiation, globally and frequently measures the physical data such as surface temperature, vegetation distribution, and ice distribution. These data might be used for acquiring the global circulation of carbon, monitoring cloud, snow, ice and sea surface temperature, and grasping the primary marine production. The GLI succeeds the mission of the Ocean Color and Temperature Scanner (OCTS) onboard the ADEOS that was launched in August, 1996, with more precision and more observation targets. The GLI has 23 channels in visible and near-infrared region (VNIR), 6 channels in short wavelength infrared region (SWIR), and 7 channels in middle and thermal infrared region (MTIR) for its multi spectral observation. The ground resolution is 1km at the nadir, a part of the channels in VNIR and SWIR has a resolution of 250m at the nadir which are used for observing vegetation and clouds. The observation region by mechanical scanning is 12 or 48 pixels (12km) in the along-track direction and 1600km in the cross-track direction. The cross track scanning is performed mechanically by rotating the scan mirror. It has also the tilting function for preventing sun glint. The tilting angle is about +20 degree or -20 degree from the progressing direction.

type	Sun-synchronous sub-recurrent orbit		
altitude	802.92 km	inclination	98.62 deg
period	101 minutes	recurrent period	4 days

Table 1 Orbit of ADEOS-II

The GLI data are received at the Earth Observation Center (EOC) of JAXA, and processed to standard products. They are transferred to the EORC for generating higher level products.

1.2 Scan Geometry of GLI

The GLI scans the geo-surface from the East to the West. The light from the Earth is reflected on the scan mirror, and reflected on 45 deg. mirror, main mirror and sub mirror, then reached the detectors as shown in Figure 1 (JAXA/EORC, 2003). The detectors are arrayed on five different focal planes (refer to Figure 2). Both sides (A and B) of the scan mirror are used for scanning. The difference of normal vectors of both sides results in the different distortion on the image.

Finally, the view vector (b_x, b_y, b_z) in the satellite coordinates is expressed by the function of following parameters.

$$(b_x, b_y, b_z) \equiv f(\omega, \theta, m, n, A/B, a, s) \quad (1)$$

where ω = scan angle
 θ = tilt angle
 (m, n) = detector address
 A/B = difference of mirror A/B side
 a = alignment for scanning axes
 s = Sat/GLI alignment

* Corresponding author.

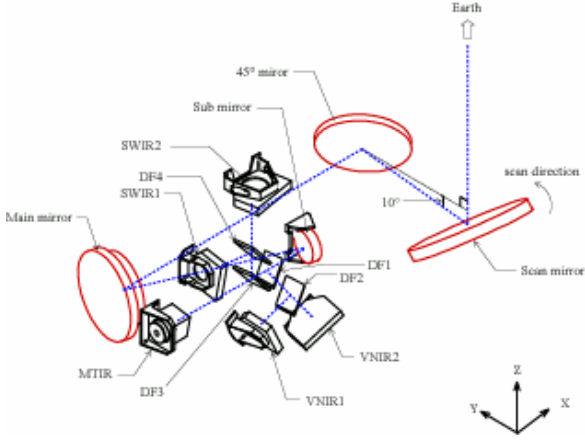


Figure 1 Optics of GLI Sensor in the Satellite Coordinates

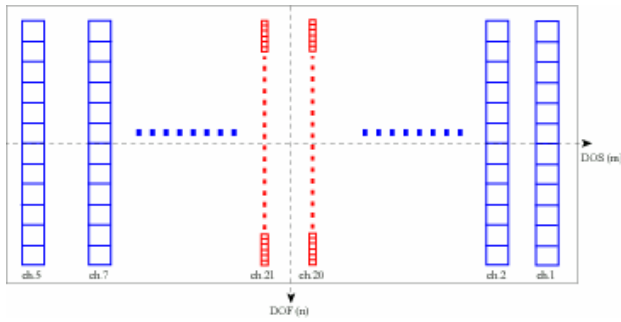


Figure 2 Example of Detectors on Focal Plane (250m, 1km)

focal plane	channel No.	
	1km	250m
VN1	1 – 9	20, 21
VN2	10 – 19	22, 23
SW1	24 – 27	
SW2		28, 29
MT	30 – 36	

Table 2 Channels of GLI

In this work, the ECR (Earth Centred Rotating) coordinates are used as the object coordinate system. The view vector in the satellite coordinates can be related with the observed object on the ECR coordinates by the following collinearity equations.

$$\begin{pmatrix} R_x \\ R_y \\ R_z \end{pmatrix} \equiv \begin{pmatrix} a_1 & a_2 & a_3 \\ a_4 & a_5 & a_6 \\ a_7 & a_8 & a_9 \end{pmatrix} \begin{pmatrix} X - X_0 \\ Y - Y_0 \\ Z - Z_0 \end{pmatrix} \quad (2)$$

$$\begin{pmatrix} a_1 & a_2 & a_3 \\ a_4 & a_5 & a_6 \\ a_7 & a_8 & a_9 \end{pmatrix} = \mathbf{P}^t \quad (3)$$

$$\begin{cases} F_x = b_x - b_z \frac{R_x}{R_z} = 0 \\ F_y = b_y - b_z \frac{R_y}{R_z} = 0 \end{cases} \quad (4)$$

where (X_0, Y_0, Z_0) = satellite position
 (X, Y, Z) = object coordinates in ECR coordinates
 \mathbf{P} = transformation matrix from satellite coordinates to ECR coordinates

The matrix \mathbf{P} at any time is determined by the satellite motion and attitude. The products of the GLI contain the position and velocity in the ECI (Earth Centred Inertial) coordinates as well as the attitude of every scan.

2. CORRECTION PROCEDURE

2.1 GCP Extraction

The correction procedure is conducted utilizing a Ground Control Point (GCP). The GCPs are extracted automatically by the template matching as shown in Figure 1. About 1,000 GCP candidates are selected from the capes or islands all over the world and stored in the library. As the coastal data base, the GSHHS (Global Self-consistent, Hierarchical, High-resolution Shoreline database) prepared by Univ. of Hawaii are used (Wessel, 1999). The matching procedure can be done with sub-pixel unit. In this work, the size of 1/4 pixel was adopted. Besides of the pair of object coordinates and image coordinates of each GCP, the GCP data set contains the errors derived by the subtraction of estimated image coordinates (L_e, P_e) from actual image coordinates (L, P). The GCP data sets are made by different process levels (or different parameters) as shown in Table 3. Although most of the GCPs are from the non-tilt operation, some GCPs are from the tilt operation.

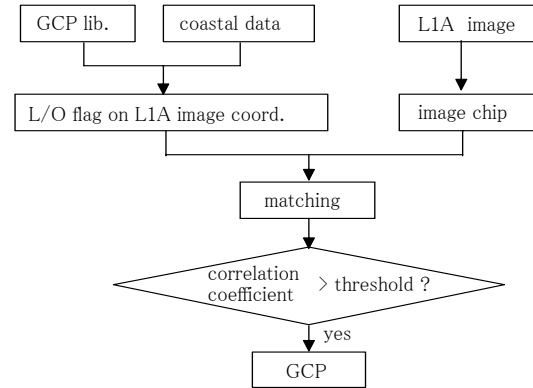


Figure 3 Automatic GCP Extraction

res.	name	level*	remarks	
			No.	channels
250m	Q1	a	678	23
	Q2	b	251	all
	Q3	c	1719	all
	Q4	d	2034	all
1km	K1	a	3418	19,24,26,30,34,35,36
	K2	b	13574	all (except 31, 32, 33)
	K3	d	12499	all (except 31, 32, 33)

*) a: just after launch
 b: after correction of Sat/GLI alignment
 c: after modification of detector address
 d: after all corrections

Table 3 GCP Data Sets

2.2 Correction of Sat./GLI Alignment

At first, the geometric accuracy just after the launch was evaluated by utilizing the GCP data set. As an example, the case of ch.23 (250m channel) is shown in Figure 4. The errors in the along-track (line) direction are proportional to pixel number, while those in the cross-track (pixel) direction are almost same. Such error pattern is very similar to that of the case of attitude error, where the linearly changed line errors are induced by pitch and yaw error, and the pixel errors are by roll error. Among the parameters related with the view vector, only the alignment of the GLI sensor against the satellite (denoted as ‘Sat/GLI alignment’) has the same effect on the image as the attitude. The components of the alignments are denoted as (α , β , γ) which correspond to roll, pitch, yaw angle, respectively.

By the Taylor’s expansion of the collinearity equations with unknown parameters, the observation equations are written as follows.

$$\begin{cases} F_x^o + v_x - \frac{\partial F_x}{\partial \alpha} - \frac{\partial F_x}{\partial \beta} - \frac{\partial F_x}{\partial \gamma} = 0 \\ F_y^o + v_y - \frac{\partial F_y}{\partial \alpha} - \frac{\partial F_y}{\partial \beta} - \frac{\partial F_y}{\partial \gamma} = 0 \end{cases} \quad (5)$$

where (F_x^o, F_y^o) = initial approximation,
 (v_x, v_y) = residuals

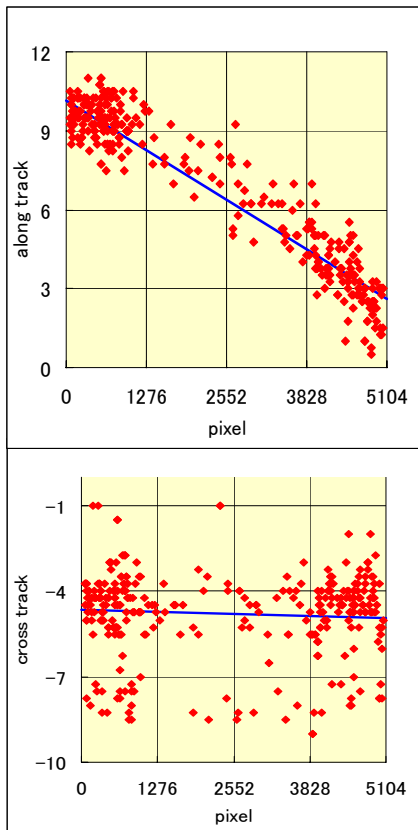


Figure 4 Geometric Accuracy just after Launch (ch.23, mirror_A)

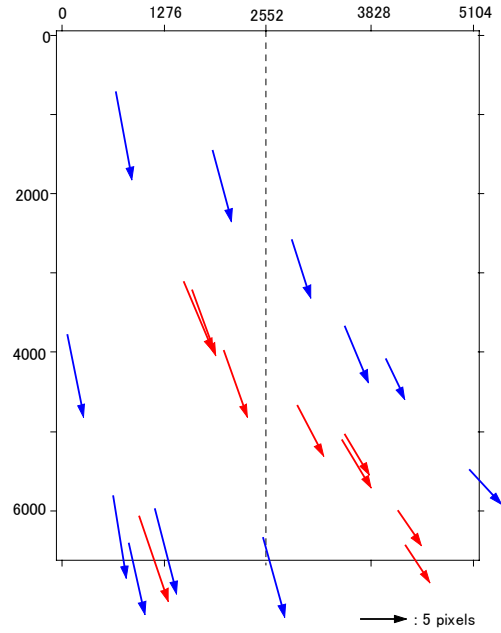


Figure 5 Example of Error Pattern of the Product just after Launch (ch.23, mirror_A)

The orientations were tried using the various GCP data sets; different resolution data, different scan mirror side, etc. As the result, the residuals from mirror A and B could not be treated as the same. The extracted alignments from the GCP sets of 250m channel and those of 1km channel could not be treated as the same. Table 4 shows the corrected alignments from the GCP sets of mirror A with different resolution as well as the values of pre-flight test (PFT). The result from the mirror A of GCP sets of 250m channel data is adopted.

res.	GCP	α	β	γ
PFT		0.02583	-0.00819	0.02083
250m	Q1	0.078145	0.115873	0.075058
1km	K1	0.121208	0.098561	0.074197

Table 4 Corrected Sat/GLI Alignment (deg.)

2.3 Modification of Detector Address

The corrected values of the Sat/GLI alignment are installed to the EOC processing system. The GCP data sets (Q2 and K2) are made with the new system. The geometric accuracy of the products by the new system is evaluated with the data sets. The mean values of the errors are shown in Figure 6. They vary with channel number.

For the correction of the dependency of errors on channel number, the addresses of detectors on the focal plane are modified. The examples of correction values for modification are shown in Table 5.

250m	Q2	Ch.20	Ch.23	Ch.29
		0.80 -0.12	-0.76 0.12	0.04 0.20
1km	K2	Ch.19	Ch.24	Ch.34
		-0.80 -0.10	0.16 0.04	0.00 -0.04

Table 5 Modified Address (Δm , Δn) (partial)

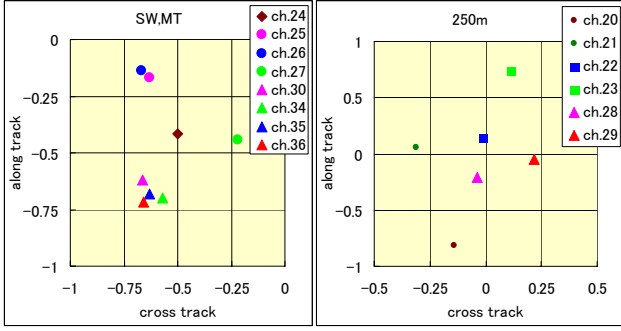


Figure 6 Geometric Accuracy after the Correction of Sat/GLI Alignment (mean error, unit: pixel)

2.4 Correction of Difference of Mirror A/B

Even though the corrections mentioned above are done, the errors for mirror A and B are different from each other. The parameter “A/B” is only related with the difference of scan mirror A and B. So this parameter should be corrected on next step. The difference of mirror A/B side is expressed by the angle (δ_1, δ_2) around the scanning axis. The angle is defined by relative values to side A. In other words, the effect of those parameters appears only on the image scanned by the mirror B. Such a difference has the effect of distortion on the image as shown Figure 7.

Similar to the equation (5), the observation equations are written as follows. The correction values as shown in Table 6 were acquired by the orientation using the GCP data set (Q3).

$$\begin{cases} F_x^o + v_x - \frac{\partial F_x}{\partial \delta_1} - \frac{\partial F_x}{\partial \delta_2} = 0 \\ F_y^o + v_y - \frac{\partial F_y}{\partial \delta_1} - \frac{\partial F_y}{\partial \delta_2} = 0 \end{cases} \quad (6)$$

	Mirror A		Mirror B		B - A	
	V_L	V_P	V_L	V_P	V_L	V_P
ch.23	-0.026	.058	.017	-.702	.044	-.760
ch.28	-.116	.091	-.072	-.672	.044	-.763
ch.29	-.135	.065	-.084	-.613	.052	-.678

Table 6 Difference of Errors for Mirror A/B (partial, used GCP: Q3, unit: pixel)

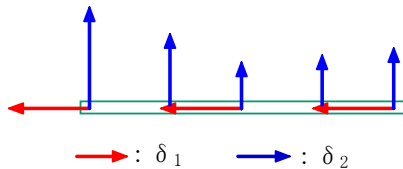


Figure 7 Effect of Mirror A/B Difference on Image

GCP	δ_1	δ_2
Q3	-11.6	37.4

Table 7 Corrected Mirror_A/B Difference (arcsec.)

2.5 Geometric Accuracy after All Corrections

Through up to section 2.4, the parameters of Sat./GLI, detector address, the difference of Mirror A & B concerning the view vector were corrected. The geometric accuracy after all corrections was evaluated using GCP data sets of Q4 and K3.

The results of some channels are shown in Table 8. In the table, the accuracy was evaluated by the R.M.S.E., mean errors and the difference between the mean errors from mirror A/B. As an example, the error distribution of ch.23 is shown in Figure 8. The Table 8 and Figure 8 indicate that the error differences of Mirror A/B were decreased specially in pixel direction. The geometric accuracy (1σ) by system correction will be expected about 1 pixel for 250m channel and less than one pixel for 1km channel image.

	ch	A/B	GCP	V_L	V_P	V
250 m	ch.23	A	250	0.928	0.739	1.187
		B	238	0.931	0.792	1.222
	ch.28	A	225	0.881	0.754	1.159
		B	226	0.931	0.783	1.217
1 km	ch.29	A	186	0.836	0.706	1.095
		B	181	0.868	0.789	1.173
	ch.29	A	556	0.592	0.587	0.833
		B	502	0.511	0.478	0.700
ch.29	A	591	0.558	0.483	0.738	
	B	561	0.515	0.516	0.729	
ch.29	A	372	0.510	0.543	0.745	
	B	331	0.500	0.600	0.780	

(a) R.M.S.E

	ch	A/B	V_L	V_P	B - A
250 m	ch.23	A	-0.100	0.029	.060
		B	-0.040	-0.033	-.062
	ch.28	A	-0.066	0.003	.041
		B	-0.107	-0.020	-.023
ch.29	A	-0.036	-0.101	-.047	
	B	-0.083	-0.094	.007	
1 km	ch.19	A	-0.024	0.015	.032
		B	0.008	0.028	.013
	ch.24	A	-0.045	0.016	.036
		B	0.009	0.030	.014
ch.34	A	0.027	0.019	-.041	
	B	-0.014	0.019	-.000	

(b) Mean Errors and Difference of Mirror_A/B

Table 8 Geometric Accuracy after All Corrections (used GCP set: Q4, K3, unit: pixel)

3. CONCLUSION

The processing system at the EOC for geometric correction was modified on the following three steps.

- 1) The alignment of the GLI sensor against the satellite (Sat/GLI alignment) was corrected on the base of photogrammetry by using the collinearity equations.
- 2) The addresses of detectors on the focal plane were modified for the correction of the dependency of errors on channel number.
- 3) The difference of mirror A/B side was corrected by using the collinearity equations, too.

The geometric accuracy just after the launch was a few kilometers on the ground. By the modification of processing system at the EOC, the accuracy was improved so that it will be expected about 1 pixel for 250m channel and less than one pixel for 1km channel image.

For the GLI products in which a higher accuracy is needed like image composites, the precise geometric correction will be conducted scene by scene using GCPs, where the satellite attitude is treated as unknown. If a few GCPs are acquired for one scene, the geometric accuracy of 250m image will be less than one pixel.

Unfortunately, the ADEOS-II satellite was terminated on October 2003. The lifetime was only about ten months. It became impossible to monitor the earth environments in long term, however, the data acquired in the operational term are very important for various researches on the Earth Science. Those data are processed to higher level products like vegetation indices, SST, ocean colors, optical thickness, etc.

References:

JAXA/EORC, 2003, "ADEOS-II - Reference Handbook -", http://sharaku.eorc.jaxa.jp/ADEOS2/doc/document_j.html (accessed 28 April. 2004)

Paul Wessel, 1999, "GSHHS - A Global Self-consistent, Hierarchical, High-resolution Shoreline database -", <http://www.soest.hawaii.edu/wessel/gshhs/gshhs.html> (accessed 28 April. 2004)

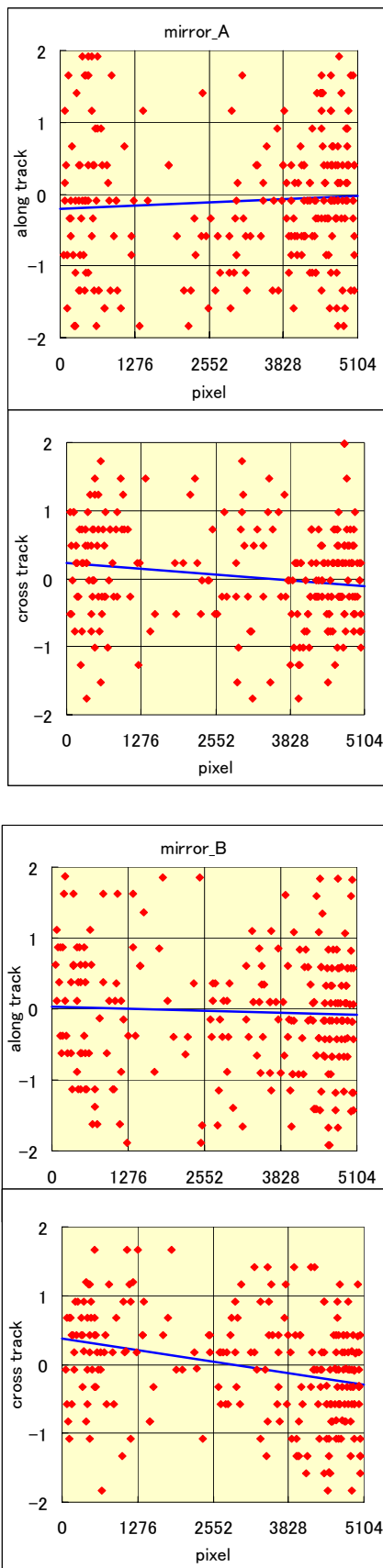


Figure 8 Geometric Accuracy after All Corrections (ch.23, mirror A and B)